

Variations of Lake Ice Phenology on the Tibetan Plateau from 2001 to 2017 Based on MODIS Data

Yu Cai^{1,2,3}, Chang-Qing Ke^{1,2,3,4,*}, Xingong Li⁵, Guoqing Zhang⁶, Zheng Duan⁷,
Hoonyol Lee⁸

1. School of Geography and Ocean Science, Nanjing University, Nanjing, 210023, China
2. Jiangsu Provincial Key Laboratory of Geographic Information Science and Technology, Nanjing University, Nanjing, 210023, China
3. Key Laboratory for Satellite Mapping Technology and Applications of State Administration of Surveying, Mapping and Geoinformation of China, Nanjing University, Nanjing, 210023, China
4. Collaborative Innovation Center of Novel Software Technology and Industrialization, Nanjing, 210023, China
5. Department of Geography and Atmospheric Science, The University of Kansas, Lawrence, KS 66045-7316, USA
6. Institute of Tibetan Plateau Research, Chinese Academy of Sciences, Beijing, 100101, China
7. Technical University of Munich, Munich, 80333, Germany
8. Division of Geology and Geophysics, Kangwon National University, Chuncheon, Kangwon-do 24341, Republic of Korea

*Corresponding author: Chang-Qing Ke (C. Q. Ke, kecq@nju.edu.cn)

Tel: 0086-25-89685860

Fax: 0086-25-83592686

Key Points:

- Lakes in the northern Inner Tibetan Plateau (Inner-TP) have longer ice cover durations than those in the southern Inner-TP.
- 18 lakes have extending ice cover durations (avg. 1.11 d yr⁻¹) and 40 lakes have shortening durations (avg. 0.80 d yr⁻¹).
- Lake ice phenology is influenced by climatic conditions, geographical location, and the physico-chemical characteristics of the lakes.

30 **Abstract**

31 Lake ice is a robust indicator of climate change. The availability of information contained in
32 Moderate Resolution Imaging Spectroradiometer (MODIS) daily snow products from 2000 to
33 2017 could be greatly improved after cloud removal by gap filling. Thresholds based on open
34 water pixel numbers are used to extract the freeze-up start and break-up end dates for 58 lakes on
35 the Tibetan Plateau (TP), 18 lakes are also selected to extract the freeze-up end and break-up
36 start dates. The lake ice durations are further calculated based on freeze-up and break-up dates.
37 Lakes on the TP begin to freeze-up in late October and all the lakes start the ice cover period in
38 mid-January of the following year. In late March, some lakes begin to break-up, and all the lakes
39 end the ice cover period in early July. Generally, the lakes in the northern Inner-TP have earlier
40 freeze-up dates and later break-up dates (i.e. longer ice cover durations) than those in the
41 southern Inner-TP. Over 17 years, the mean ice cover duration of 58 lakes is 157.78 days, 18
42 (31%) lakes have a mean extending rate of 1.11 d yr^{-1} and 40 (69%) lakes have a mean
43 shortening rate of 0.80 d yr^{-1} . Geographical location and climate conditions determine the spatial
44 heterogeneity of the lake ice phenology, especially the ones of break-up dates, while the physico-
45 chemical characteristics mainly affect the freeze-up dates of the lake ice in this study. Ice cover
46 duration is affected by both climatic and lake specific physico-chemical factors, which can
47 reflect the climatic and environmental change for lakes on the TP.

48 **Key Words:** Lake ice phenology; Freeze-up/break-up dates; Climate change; MODIS; Tibetan
49 Plateau

50

51

52

53 **1 Introduction**

54 There are about 1200 lakes (>1 km²) on the Tibetan Plateau (TP) (Zhang, Yao, Xie, Zhang,
55 K., et al., 2014) and many studies have shown that lake ice phenology (i.e., the timing of freeze-
56 up, break-up and duration of ice cover) responds well to climatic and environmental changes
57 (Brown & Duguay, 2010; Weber et al., 2016). As “the Third Pole of the Earth”, the TP is very
58 sensitive to global climate change (Liu & Chen, 2000; Qiu, 2008; Kang et al., 2010). Changes in
59 air and water surface temperatures related to climatic changes are important factors in the lake
60 ice phenology changes (Adrian et al., 2009; Zhang, Yao, Xie, Qin, et al., 2014; Dörnhöfer &
61 Oppelt, 2016; Yao et al., 2016). At the same time, the state and type of lake ice and their change
62 to open water system in turn affects the local or regional climate (Rouse et al., 2005; Brown &
63 Duguay, 2010). Freeze-up/break-up processes can result in sudden changes in lake surface
64 properties (such as albedo and roughness), which affect the energy exchange between the lake
65 water and the atmosphere (Latifovic & Pouliot, 2007). Therefore, in the context of global climate
66 change, lake ice phenology can be used as a good indicator to monitor the actual impact of
67 climate change on lakes and their surroundings (Ke et al., 2013).

68 However, due to the harsh environment and limited accessibility, few meteorological
69 stations exist in the central and western TP, which is where lakes are concentrated; thus, it is
70 difficult to carry out field observations. These factors result in a lack of continuous and complete
71 historical records on regional climate changes (Liu & Chen, 2000; Kropacek et al., 2013).
72 Remote sensing data have been widely used in lake ice monitoring (Wei & Ye, 2010; Duguay et
73 al., 2015). Passive microwave sensors such as the Scanning Multichannel Microwave
74 Radiometer (SMMR), the Special Sensor Microwave/Image (SSM/I), and the Advanced
75 Microwave Scanning Radiometer for the Earth Observing System (AMSR-E) have high

76 temporal resolutions (at times twice daily or better) and are suitable for monitoring lake ice
77 changes in large lakes, such as Qinghai Lake (Che et al., 2009; Cai et al., 2017) and Nam Co (Ke
78 et al., 2013) on the TP, and Great Bear Lake and Great Slave Lake (Howell et al., 2009) in
79 Canada. However, there are still many medium- and small-size lakes on the TP, which are
80 smaller than the pixel size of passive microwave images (dozens to hundreds of km²). Active
81 microwave sensors have high spatial resolutions (1 m to about 100 m). For example, the
82 European Remote Sensing Satellite (ERS)-1/2 Synthetic Aperture Radar (SAR) has been used
83 for monitoring the lake ice formation process and ice thickness (Jeffries et al., 1994; Morris et
84 al., 1995; Duguay & Lafleur, 2003). Radarsat-1/2 SAR has also been used for monitoring the
85 freeze-up/break-up processes of lake ice (Duguay et al., 2002; Geldsetzer et al., 2010). However,
86 the low temporal resolution (five to six days) of the available active microwave technologies
87 limits the ability to achieve daily monitoring on lake ice (Latifovic & Pouliot, 2007; Chaouch et
88 al., 2014). The medium- and high-resolution optical data, such as Moderate Resolution Imaging
89 Spectroradiometer (MODIS) and Advanced Very High Resolution Radiometer (AVHRR) obtain
90 daily images and are often used to monitor lake freeze-up/break-up dates and areas. For example,
91 Weber et al. (2016) used AVHRR data to extract the ice phenology of European lakes in
92 different climatic regions. Yao et al. (2016) used MODIS and Landsat data to extract the ice
93 phenology of 22 lakes in the Hoh Xil region from 2000 to 2011 and analyzed the factors
94 influencing lake ice changes. Chaouch et al. (2014) used MODIS data to monitor the growth and
95 regression of ice in the Susquehanna River in the northeastern USA. However, optical images are
96 obscured by clouds, which limits the direct usage of optical data (Gafurov & Bárdossy, 2009).
97 Currently, there have been many mature cloud removal methods, including methods based on
98 temporal and spatial continuity (Gafurov & Bárdossy, 2009; Paudel & Andersen, 2011; López-

99 Burgos et al., 2013) and methods combining multiple sensor data (Liang et al., 2008; Gao, Xie,
100 Lu, et al., 2010; Gao, Xie, Yao, et al., 2010), which can reduce cloud cover and increase data
101 availability by gap filling approaches and compositing.

102 The unique geographical and climatic conditions of the TP make it a region of high interest
103 for climate research (Kang et al., 2010). Owing to the low annual air temperature, many lakes on
104 the TP have long and stable ice cover periods during winter. Recent studies on individual lakes
105 have shown that on the TP, the freeze-up dates of some lakes have been delayed, the break-up
106 dates have advanced, and the ice cover durations have significantly shortened (Che et al., 2009;
107 Ke et al., 2013; Cai et al., 2017). However, there are few ice phenology studies covering the
108 entire TP. Guo et al. (2018) used MODIS reflectance data, eight-day synthetic snow product and
109 land surface temperature data to analysis the uncertainty and variation of different remotely
110 sensed lake ice phenology across the TP. Kropáček et al. (2013) used MODIS eight-day
111 synthetic snow products to analyze the ice phenology changes of 59 large lakes on the TP from
112 2001 to 2010. However, the eight-day interval could not capture the lake ice phenology very
113 precisely, especially for the start and end dates of freeze-up and break-up. To date, no one has
114 used MODIS daily snow products to study the lake ice phenology on the TP.

115 To obtain the lake ice phenology variations on the TP, the daily snow products of MODIS
116 are used to extract the freeze-up and break-up dates of lake-wide ice cover from 2001 to 2017.
117 The lake ice durations are then calculated, and the spatial variabilities and change rates of lake
118 ice phenology are analyzed. Using reanalysis data and available satellite data set, the effects of
119 air temperature, lake surface water temperature, and wind speed on lake ice phenology are
120 analyzed. In addition, possible influence of geographical determined lake locations and physico-
121 chemical conditions on lake ice phenology are also investigated.

122 **2 Study area**

123 The TP is located in central Asia; it is the largest plateau in China, and its elevation is the
124 highest in the world. The TP is known as the “roof of the world” and “the Third Pole of the
125 Earth”, with an average elevation of over 4,000 m a.s.l and a total area of approximately 3.0
126 million km² (Qiu, 2008; Zhang et al., 2013). There are about 1,200 lakes (>1 km²) on the TP
127 with a total size of 47,000 km², which accounts for more than 50% of the total size of Chinese
128 lakes (Zhang, Yao, Xie, Zhang, K., et al., 2014), in which 389 lakes have an area larger than 10
129 km², including three lakes larger than 1,000 km²: Qinghai Lake (4,254.9 km²), Selin Co
130 (2,129.02 km²) and Nam Co (2,040.9 km²) (Wan et al., 2014).

131 By analyzing the change of ice coverage for each lake using MODIS daily snow products,
132 58 lakes with a stable ice cover period (less cloud cover, less pixel misclassification and obvious
133 ice cover period) are manually selected as study lakes (Figure 1), including three lakes larger
134 than 1,000 km², 35 lakes larger than 100 km² and 20 lakes smaller than 100 km², in which the
135 smallest lake is Xuemei Lake (41.33 km², Wan et al., 2014). Most lakes (>70%) are in the Inner
136 basin (Zhang et al., 2013). To analyze the spatial variability of lake ice phenology, the Inner
137 basin is divided into upper and lower parts (Inner I and Inner II, northern and southern parts of
138 about 33°N) (Zhang et al., 2013), and lakes outside the Inner basin are classified as Other III
139 (Figure 1). The lake masks used were extracted from Landsat images (Wan et al., 2014) and all
140 data sets involved in the extraction and comparisons are clipped by the same lake mask. An
141 annual period extends from 1 August to 31 July of the following year, for example, 1 August
142 2012 to 31 July 2013 is noted as the annual period of 2013.

143 **3 Data and methods**

144 **3.1 Data**

145 *3.1.1 MODIS daily snow cover products*

146 MODIS is mounted on the Terra and Aqua satellites, which obtain global observation data
147 every one or two days. The available daily snow cover products with a spatial resolution of 500
148 m from MODIS include MOD10A1 (Terra) and MYD10A1 (Aqua). The available temporal
149 range of MOD10A1 is from 1 August 2000 to 31 July 2017 and that of MYD10A1 is from 1
150 August 2002 to 31 July 2017. Four MODIS tiles (h24v05, h25v05, h25v06 and h26v05) cover
151 the 58 lakes of this study. The data were obtained from the US National Snow and Ice Data
152 Center (<http://nsidc.org/>, Version 5 for 2001-2016 and Version 6 for 2017) on 8 September 2017.

153 The accuracy of the daily snow cover products of MODIS are approximately 93% under
154 clear sky conditions (Maurer et al., 2003; Parajka & Blöschl, 2006; Hall & Riggs, 2007; Sorman
155 et al., 2007; Huang et al., 2011). However, the daily snow cover products over the TP have a
156 yearly average cloud cover (>40%) from MODIS observations (Yu et al., 2016), and need to be
157 processed for cloud removal by gap filling. Some lakes may have snow covering the ice surface
158 during the ice cover period, and MODIS snow cover products could classify these ice covered
159 pixels into snow covered pixels, which results in a low lake ice cover compared to the lake size
160 (Kropacek et al., 2013). Therefore, the changes of lake water cover proportions (the number of
161 lake water pixels divided by the total number of pixels within the lake boundary) are used to
162 extract the freeze-up/break-up dates, and the lake ice cover proportions are used to assist in
163 correcting the date results. Under clear sky conditions, the reduction in water cover is considered
164 as the result of lake ice cover increase.

165 *3.1.2 Landsat data*

166 The Landsat program is a series of Earth observing satellites, which is co-managed by the
167 National Aeronautics and Space Administration (NASA) and the United States Geological
168 Survey (USGS) to monitor earth and environmental resources. Since 23 July 1972, eight
169 satellites have been launched including Landsat Multispectral Scanner (MSS, ~80 m) and
170 Thematic Mapper (TM, 30m)/Enhanced Thematic Mapper Plus (ETM+, 30m)/Operational Land
171 Imager (OLI, 30 m) with a temporal resolution of 16 days. Landsat data used are from the
172 standard USGS Landsat Surface Reflectance products (Collection 1 Level-2) of Landsat 5, 7 and
173 8 from 2000 to 2017 on the Google Earth Engine platform (<https://earthengine.google.com/>).
174 Images without cloud cover and obtained during the freeze-up or break-up periods are selected to
175 extract the lake water cover proportions.

176 To extract lake ice, pixels covering a lake need to be first distinguished from other types of
177 pixels, such as cloud and land. A threshold of 0.4 for Normalized Difference Snow Index (NDSI)
178 (Hall et al., 2001) is applied to extract the extent of a lake as follows:

$$179 \quad NDSI = (TM \text{ Band } 2 - TM \text{ Band } 5) / (TM \text{ Band } 2 + TM \text{ Band } 5) \geq 0.4 \quad (1)$$

180 Then, according to the actual reflectance of each image, different thresholds on the near-
181 infrared band are set to distinguish lake ice from lake water. Finally, the proportion of lake water
182 within a lake boundary (1 – ice cover proportion) is calculated and compared with MODIS
183 results on the same day to verify the accuracy of using MODIS snow cover products after cloud
184 removal by gap filling.

185 *3.1.3 Lake ice phenology products from AMSR-E/2 data*

186 The daily lake ice phenology time series derived from AMSR-E and AMSR2 by Du et al.
187 (2017) provide 5 km ice phenology retrievals describing daily lake ice conditions over the
188 Northern Hemisphere (http://files.ntsg.umt.edu/data/AMSRE2_LAKE_ICE_PHEN/). The date
189 set is used for lake-wide comparisons against MODIS data results from 2003 to 2011 and from
190 2013 to 2015. Pixels within the lake boundary are extracted for eight lakes larger than 500 km².
191 Considering the differences between passive microwave and optical data and the difference in
192 data productions, when the number of ice-on pixels count for more than 10% of all pixels in the
193 lake, the date is determined to be freeze-up start date, and less than 10% is break-up end date.

194 *3.1.4 Reanalysis meteorological data*

195 The NCEP/NCAR reanalysis data set is a joint product from the National Centers for
196 Environment Prediction (NCEP) and the National Center for Atmospheric Research (NCAR,
197 <https://www.esrl.noaa.gov/>). This data set provides reanalysis meteorological data every six
198 hours including air temperature, air pressure, relative humidity, and wind speed at a spatial
199 resolution of 2.5° from 1 January 1948 to present. The monthly mean data of near surface air
200 temperature and wind speed are used.

201 To match the annual ice period, the annual mean air temperature and wind speed are
202 calculated from August of the current year to July of the following year. Then, the change rates
203 of air temperature and wind speed from 2001 to 2017 are calculated. Finally, the inverse distance
204 weighted (IDW) method is used to interpolate and calculate the means and change rates of air
205 temperature and wind speed for each lake over the 17 years.

206 **3.2 Methods**207 *3.2.1 Cloud removal for the MODIS snow product*

208 The cloud removal (gap filling) process has two steps. The first step is to combine daily
 209 Terra and Aqua snow cover products to determine lake cover type (Gafurov & Bárdossy, 2009).
 210 For a pixel A , if any of the pixels on Terra or Aqua images for the same day is open water (or
 211 other useful pixel types such as ice and snow, the same below), the pixel on the output image is
 212 determined to be covered by water. When the pixel is covered with clouds (or other useless types
 213 such as land and missing data, the same below) on both Terra and Aqua images, the output pixel
 214 is determined to be cloud covered (Gafurov & Bárdossy, 2009):

$$215 \quad S_{(A, output)} = water \text{ if } S_{(A, Aqua)} = water \text{ OR } S_{(A, Terra)} = water \quad (2)$$

$$216 \quad S_{(A, output)} = cloud \text{ if } S_{(A, Aqua)} = cloud \text{ AND } S_{(A, Terra)} = cloud \quad (3)$$

217 Since Aqua satellite was launched in 2002, there is no first step data process for the 2001-
 218 2002 period. The images from step one are used as the inputs for the following step. The second
 219 step is based on the temporal correlation of cloud cover pixels (Gafurov & Bárdossy, 2009).
 220 First, if a pixel A on date t is cloud covered, the pixels on the images of previous and next days
 221 will be searched, and if both pixels are water covered, pixel on date t is determined to be covered
 222 by water as follows (Gafurov & Bárdossy, 2009):

$$223 \quad S_{(A, t)} = water \text{ if } S_{(A, t-1)} = water \text{ AND } S_{(A, t+1)} = water \quad (4)$$

224 If pixel A on date $t-1$ is cloud covered, then the pixel on date $t-2$ will be searched, and if
 225 both pixels on date $t-2$ and date $t+1$ are water covered, the pixels on date t and $t-1$ will be
 226 replaced by water. Similarly, if the pixel on date $t+1$ is cloud covered, the pixel on date $t+2$ will
 227 be searched as follows (Gafurov & Bárdossy, 2009):

$$S_{(A, t-1)}, S_{(A, t)} = \text{water} \text{ if } S_{(A, t-2)} = \text{water} \text{ AND } S_{(A, t+1)} = \text{water} \quad (5)$$

$$S_{(A, t)}, S_{(A, t+1)} = \text{water} \text{ if } S_{(A, t-1)} = \text{water} \text{ AND } S_{(A, t+2)} = \text{water} \quad (6)$$

3.2.2 Extraction of freeze-up/break-up dates

Often, there will be an unfrozen area near a lake's outlet during the freeze-up period, and a small amount of accumulated lake ice on the lakeshore during the break-up process (Reed et al., 2009; Yao et al., 2016). In addition, repeated freeze-up and break-up periods caused by weather changes, mismatch of lake boundaries, misclassification of pixels and inevitable noise (especially cloud cover) will all change the extraction of lake ice phenology. Therefore, Kropacek et al. (2013) proposed using 5% and 95% of the lake area as thresholds to extract ice phenology instead of 0% and 100%. Simultaneously, images with a cloud cover of more than 50% over a lake after gap filling are eliminated to reduce the influence from sudden changes in water cover.

First, a median M of all the lake water cover proportions in a year is calculated. Then, all the water cover proportions are divided into two groups: one group (G_h) contains the values greater than M , and the other group (G_l) contains the values less than M , and the mean values of both groups are calculated. Two thresholds are determined by using the 5% and 95% of the two mean values as follows (Kropacek et al., 2013):

$$Th_h = 95\% \cdot M_h + 5\% \cdot M_l \quad (7)$$

$$Th_l = 5\% \cdot M_h + 95\% \cdot M_l \quad (8)$$

Where M_h and M_l are the mean values of group G_h and G_l , respectively. Since the freeze-up/break-up processes of lakes are usually short, M_h can represent the typical proportion of a lake

250 covered by water during the non-ice cover period, and M_l can represent the typical water cover
251 proportion during ice cover period (Kropacek et al., 2013). The dates when the water cover will
252 no longer raise above the thresholds (Th_h for freeze-up start date and Th_l for freeze-up end date)
253 again during the freeze-up period and will no longer drop below the thresholds (Th_l for break-up
254 start date and Th_h for break-up end date) during the break-up period are extracted as the ideal
255 lake ice phenology dates. Sometimes the remained cloud cover (or other useless pixels) will
256 decrease the water cover (even smaller than the thresholds). Therefore, after the automatic
257 extraction, the extracted dates need to be checked again by visual interpretation of the complete
258 water, ice and cloud cover changes within a year (Figure 2).

259 The four freeze-up/break-up dates divide the annual status of a lake into four periods and
260 the corresponding durations can be calculated: freeze-up duration (FUD, from freeze-up start to
261 freeze-up end), break-up duration (BUD, from break-up start to break-up end), complete freezing
262 duration (CFD, from freeze-up end to break-up start) and ice cover duration (ICD, from freeze-
263 up start to break-up end).

264 3.2.3 Statistical analysis

265 The mean absolute error (MAE), correction of determination (R^2) and bias are measured
266 for comparisons between the MODIS cloud-removed and Landsat data as well as comparisons
267 between ice phenology results derived from MODIS and passive microwave data sets. Trend
268 significances of lake ice dates and durations are evaluated using the non-parametric Mann-
269 Kendall test (Mann, 1945; Kendall, 1975). Furthermore, the relationships between lake ice
270 phenology parameters and climate conditions are evaluated using the coefficient of correlation
271 (r).

272 **4 Results**

273 *4.1 Cloud removal of MODIS snow cover products and validation using Landsat data*

274 *4.1.1 Cloud removal by gap filling*

275 Taking the year 2013 as an example, before gap filling, the mean cloud cover of the 58
276 lakes is 44.97% and 51.70%, respectively, for Terra and Aqua. After the first step of combining
277 the data from two satellites, the cloud cover is eliminated to 31.02%. After the second step of
278 using pixels in neighboring dates, the mean cloud cover is eliminated to 16.54%. Taiyang Lake
279 has a mean cloud cover of more than 60%, which is the highest among 58 lakes, and it is
280 eliminated to 35.49% after the cloud removal. For some lakes, the cloud cover can even be
281 eliminated to less than 5% after cloud removal (Table 1). For example, the mean cloud cover of
282 Qinghai Lake in 2013 after cloud removal is 7.54%, and the freeze-up/break-up dates can be
283 clearly distinguished (Figure 2).

284 *4.1.2 Validation*

285 For some large lakes, such as Qinghai Lake, Landsat images cannot cover the entire lake on
286 the same day and images acquired from different days cannot be mosaiced to extract the lake ice.
287 Often, the freeze-up/break-up period of a lake is only a dozen of days, which is usually not
288 captured by Landsat images due to the 16-day temporal resolution. In addition, considering the
289 influence of cloud cover, there are indeed few available Landsat images. Therefore, lakes which
290 can be covered by one Landsat image and those with relatively long freeze-up/break-up period
291 are preferably selected for validation.

292 A total of 28 Landsat images covering Nam Co (19 images) and Selin Co (9 images) during
293 the freeze-up or break-up periods are selected. The proportions of lake water to total lake area

294 are calculated for each image and compared with the water cover proportions from the cloud
295 removed MODIS data. The R^2 is 0.95, the mean absolute error (MAE) is 4.58% and the bias is
296 2.09% (Figure 3), indicating a relatively high accuracy and MODIS data can be used to detect
297 lake water changes well after cloud removal.

298 ***4.2. Comparisons against other lake ice data sets***

299 Daily passive microwave brightness temperature data, including AMSR-E/2 and SSM/I, are
300 used for cross-validation with MODIS lake ice phenology results. The freeze-up start and break-
301 up end dates of eight lakes (larger than 500 km²) derived from AMSR-E/2 pixel-level lake ice
302 phenology products (Du et al., 2017) from 2003 to 2015 (except 2012) are compared with
303 corresponding MODIS dates and the results are shown in Table 2. The break-up end dates from
304 two data sets are strongly correlated (avg. $R^2 = 0.90$) but the freeze-up start dates have relatively
305 low consistency (avg. $R^2 = 0.35$). Generally, MODIS dates are earlier than AMSR dates, but vary
306 from lake to lake (Table 2). The MAEs of freeze-up start dates range for eight lakes from 2.92 to
307 7.25 days and break-up end dates range from 1.75 to 3.25 days.

308 Furthermore, ice phenology data for Qinghai Lake (from 2001 to 2016, Cai et al., 2017) and
309 Nam Co (from 2001 to 2013, Ke et al., 2013) derived from SSM/I data are also compared with
310 MODIS results. The correlations of freeze-up start and break-up end dates for Nam Co are low
311 ($R^2 = 0.42$ and 0.35, respectively) and the MAEs are both over six days (Table 2). The freeze-up
312 start date from MODIS data is obviously earlier than SSM/I data (bias = -5.28 days), this may be
313 because Nam Co only covered by two SSM/I pixels and less information can be provided. On the
314 other hand, Qinghai Lake provided four freeze-up/break-up dates for comparison against MODIS
315 data. Similar to AMSR results, the consistency of freeze-up dates are lower than break-up dates
316 (Figure 4). Moreover, in Qinghai Lake, freeze-up dates from MODIS data are earlier than

317 passive microwave data (both SSM/I and AMSR) while break-up dates are later (Figure 4), this
318 may be because of the coarser spatial resolution and less information near the boundary of
319 passive microwave data (Cai et al., 2017). The MAE of freeze-up end date is the largest (6.56
320 days) and the MAEs of break-up dates are about two days (Figure 4). These results indicate that
321 the influence from different remote sensing data and different data production processes on
322 freeze-up dates may be larger than that on break-up dates. It is similar to the results of Du et al.
323 (2017) when he compared AMSR lake ice phenology results against Canadian Ice Service (CIS)
324 and IMS data.

325 ***4.3. Ice phenology and its change of the lakes on the TP from 2001 to 2017***

326 For each of 58 lakes, freeze-up start and break-up end dates are extracted, and their
327 corresponding ice cover durations are calculated. Some lakes do not freeze-up completely in
328 winter due to mild winters, large water volume and/or high salinity (Kropacek et al., 2013), and
329 some lakes are obscured by cloud and/or misclassified pixels during ice cover period. Apart for
330 these lakes, for 18 lakes with characteristic change of water cover proportions, the freeze-up end
331 and break-up start dates are also extracted, and four lake ice durations (i.e., freeze-up duration,
332 break-up duration, complete freezing duration and ice cover duration) are calculated, such as Har
333 Lake in Figure 5. Based on the four freeze-up/break-up dates and four durations from 2001 to
334 2017, their mean values and change rates of ice phenology for the 58 lakes are shown in
335 Appendix Table A1. Additional statistics are shown in Appendix Table B1 and Table 3.

336 ***4.3.1 Freeze-up/break-up dates***

337 Around late October, Yuye Lake has begun to freeze-up, which is the earliest among 58
338 lakes. After Taro Co had begun to freeze-up by mid-January of the following year, all the lakes

339 on the TP have started their ice cover periods. The gap between freeze-up start dates among the
340 lakes can be as long as three months. From late March to early July, the lakes have ended their
341 ice period one after another, and the earliest and latest lakes are Tuosu Lake and Gozha Co,
342 respectively. Generally, the spatial difference in the freeze-up dates are smaller than the break-up
343 dates (Table B1). The mean freeze-up start date for the lakes in the Inner I is 32.68 days earlier
344 than that of the lakes in the Inner II, while the mean break-up end date in the Inner I is 43.56
345 days later than that in the Inner II (Figure 6, Table 3).

346 Freeze-up/break-up dates for many lakes on the TP have obvious change tendencies from
347 2001 to 2017 (Table A1). For example, the freeze-up start and freeze-up end dates for Har Lake
348 have been delayed at a rate of 0.66 d yr^{-1} and 0.35 d yr^{-1} , respectively, and the break-up start and
349 break-up end dates have advanced at rates of 0.38 d yr^{-1} and 0.12 d yr^{-1} , respectively (Figure 5).
350 Overall, the change rates of freeze-up dates for most lakes are more significant than the break-up
351 dates (Table A1). Except for a few lakes in the eastern Inner I which have advancing trends in
352 the freeze-up dates, most of the lakes (81.03%) show delayed trends from 2001 to 2017. All the
353 lakes in the Inner II have delayed trends during the 17 years (Figure 6b, Table 3). Among the 58
354 lakes, the lakes with delayed and advancing trends of break-up dates are both 50% (Table 3).
355 Spatially, the delayed trend is more pronounced than the advancing trend (Figure 6d). Lakes in
356 the Inner I, such as Dogaicoring Qangco and Lexiewudan Co (change rates of the break-up end
357 dates are 3.50 d yr^{-1} and 4.25 d yr^{-1} , respectively, Table A1), experienced the most dramatic
358 changes (Figure 6d). During the 17 years, 60.34% of the lakes show an opposite change trend of
359 freeze-up and break-up dates, and another 36.21% of the lakes show the same delayed change
360 trend. Only Huolunuo'er and Meiriqiecuomari have the same advancing trend of freeze-up and
361 break-up dates (Table A1).

362 *4.3.2 Lake ice durations*

363 Lake ice cover durations on the TP differ greatly, where the duration of the shortest lake
364 (Taro Co) is less than three months, and that of the longest lake (Xuemei Lake) is approximately
365 eight months (Table B1). The spatial distribution of the ice cover duration is consistent with that
366 of the freeze-up/break-up dates: the lakes in the Inner II with later freeze-up and earlier break-up
367 have shorter ice cover durations, and the lakes in the Inner I with earlier freeze-up and later
368 break-up have longer ice cover durations (Figure 7a), which is 2 months longer on average than
369 those of the Inner II (Table 3). Among the 18 lakes extracted complete four freeze-up/break-up
370 dates, most lakes (72.2%) have shorter freeze-up durations than break-up durations, i.e., freeze-
371 up takes place faster than break-up does (Table A1). However, the variations in freeze-up
372 durations among the lakes is larger than that in break-up durations (Table B1). Among the 18
373 lakes, Hoh Xil Lake has the earliest freeze-up end date and the latest break-up start date; thus,
374 the longest complete freezing duration is up to seven months. Qinghai Lake has the shortest
375 complete freezing duration of less than three months (Table B1).

376 Over the 17 years, most of the lakes (68.97%) display a shortening trend in ice cover
377 duration. For example, Har Lake has a shortening trend of 0.77 d yr^{-1} (Figure 5d). Lakes with
378 extending trends are mainly concentrated in the eastern part of the Inner I (Figure 7b). Since all
379 the lakes in the Inner II have delayed trends of freeze-up start dates, most lakes (87.50%) have
380 their ice cover durations shortened. Similar to freeze-up/break-up dates, half of the lakes in the
381 Inner I have shortening ice cover durations and the other half have extending durations (Table 3).
382 The trends of complete freezing duration for the 18 lakes are mainly consistent with the trends of
383 ice cover duration. Lakes such as Hoh Xil Lake and Tu Co have a shortening freeze-up and
384 break-up durations, despite an extending ice cover duration. Although lakes such as Dagze Co

385 and Ngangze Co have shortening trends of ice cover duration, their shortening freeze-up and
386 break-up duration results in an extending trend of complete freezing duration. 77.78% of the
387 lakes show the same trend in freeze-up and break-up durations (Table A1). There are several
388 lakes, such as Har Lake, which have shortening freeze-up durations and extending break-up
389 durations (Figure 5c). The freeze-up and break-up durations of most lakes (both 72.2%) have
390 shortened over 17 years, which indicates that freeze-up/break-up takes place faster (Table A1).

391 **5 Discussions**

392 *5.1 Uncertainty analysis*

393 Errors in the extraction of the ice phenology from MODIS snow cover products mainly
394 come from three aspects: (1) The MODIS snow cover products have cloud cover,
395 misclassification and occasional missing data; (2) changes to the original data caused by cloud
396 removal; and (3) misjudgment when extracting the lake ice phenology dates. While the quality of
397 MODIS snow cover products cannot be changed, the proportion of usable pixels can be
398 increased by removing some of the cloud cover by gap filling. Combining Terra and Aqua data
399 can solve the problem of missing dates, and combined with the temporal information of cloud
400 (noise) covered pixels, about two-thirds of the cloud and other noise pixels can be eliminated.
401 Cloud cover could reflect most of the solar radiation, so the cloud cover in a short period of time
402 would not have much impact on lake surface coverage (Gafurov & Bárdossy, 2009). Possible
403 increased lake ice caused by snowfall during cloudy days (or low temperature at night) are
404 ignored if they break-up on the following sunny day (or in the daytime). According to the study
405 of Gafurov and Bárdossy (2009), the performance accuracy of the gap filling approach is more
406 than 95%. To maintain with the original MODIS information as much as possible, the cloud-

407 removal process only considers the temporal information one to two days before and after the
408 current day, and the potential error can be controlled within two days. Although the possible
409 error in the gap filling process is minimized, the remained and persistent (longer than two days)
410 cloud cover will still influence the extraction of ice phenology dates.

411 The remained cloud cover (or other useless pixels) will decrease the lake water/ice cover of
412 the day, and sometimes the automatic extraction method may obtain a wrong date. However,
413 these mistakes can be modified by later manual correction of comparing the complete
414 water/ice/cloud curves of that year. Using thresholds can control the difficulty caused by
415 repeated freeze-up and break-up of lake ice and ensure the consistency of the freeze-up/break-up
416 date extractions. For example, there were several periods of repeated freeze-up and break-up at
417 the start of the break-up process in Qinghai Lake in 2013. It is difficult to determine which
418 break-up date should be extracted without using a threshold. Though the extracted date seems
419 like a wrong date, the ice cover has definitely dropped after that day, so the date is determined to
420 be the break-up date of that year (Figure 2). Although some dates will be checked and modified
421 after automatic extraction, the alternative dates are all selected by the thresholds. Considering the
422 existence of noise, the thresholds are set to 5% and 95% instead of the extreme values. This
423 approach may cause the later extraction of the freeze-up start and break-up start dates, and earlier
424 of the freeze-up end and break-up end dates. But without available validation data, the actual
425 error cannot be accurately evaluated. However, the same rule is applied to all the lakes and in all
426 the years, which makes the comparisons between lakes and years possible.

427 The persistent cloud cover is difficult to be eliminated. But similarly, without surface
428 observation data, the errors cannot be accurately evaluated. It seems some lakes have the feature
429 that cloud covered most areas during freeze-up and/or break-up periods. However, lakes with too

430 much noise or complex shape (for example, Bangong Co is long and narrow and Yamzho
431 Yumco is tentacle-like) that cannot guarantee the reasonable dates has already been excluded in
432 the lake selection period. Furthermore, some lakes have persistent cloud cover after they begin to
433 freeze-up, it is probably caused by misclassification of ice to cloud. If the cloud cover influences
434 the extraction of the freeze-up end and/or break-up start date, the dates will not be extracted.
435 Only lakes with clear curves of water/ice changes are chosen in order to obtain more accurate
436 dates, even if the cost is that the number of the study lakes will be reduced.

437 Kropáček et al. (2013) extracted the lake ice phenology of 59 large lakes on the TP from
438 2001 to 2010 using MODIS eight-day synthetic snow products. The lakes were divided into three
439 groups, among which the lakes in Group C were almost all located in the Inner II. The mean ice
440 cover duration of lakes in Group C was 126 days with a shortening trend of 1.6 d yr^{-1} , while the
441 mean ice cover duration of lakes in the Inner II in this study is 128 days from 2001 to 2017, and
442 the mean change rate of 21 lakes is -0.89 d yr^{-1} . The two mean ice cover durations are similar,
443 the change trends are consistent, and the lower rate in this study may be caused by gentler
444 change in recent years. Yao et al. (2016) used MODIS and Landsat data to study lake ice
445 phenology in the Hoh Xil region from 2000 to 2011. Their mean ice cover duration was 196 days
446 with a mean change rate of -1.91 d yr^{-1} . The Hoh Xil region is in central Inner I, and the lakes
447 analyzed in their study include Dogaicoring Qangco, Taiyang Lake, Hoh Xil Lake, Lexiewudan
448 Co, and Margai Caka. This is the region where lake ice phenology has changed drastically in
449 recent years within the TP (Figure 6). Consistent with the results of this study, Dogaicoring
450 Qangco and Lexiewudan Co are the rare lakes in this region with advancing freeze-up dates and
451 delayed break-up dates, and the reason for these changes will be discussed in the following
452 section. However, in this study, the freeze-up start and break-up end dates of Taiyang Lake have

453 been delayed over 17 years, which is different from an advancing break-up end date in Yao et al.
454 (2016). From 2000 to 2011, the break-up end date of Taiyang Lake did show an advancing trend
455 with a rate of 1.51 d yr^{-1} . However, since 2010, the break-up end date has been delayed annually
456 with a change rate of 3.23 d yr^{-1} until 2017, which results in an overall delayed trend from 2001
457 to 2017. Furthermore, many studies have shown that some large lakes on the TP such as Qinghai
458 Lake and Nam Co show a significant delayed trend in freeze-up dates and an advancing trend in
459 break-up dates, and the ice cover durations have shortened in recent years (Che et al., 2009; Ke
460 et al., 2013; Cai et al., 2017), which is consistent with the results of this study.

461 ***5.2. Influencing factors on lake ice phenology***

462 *5.2.1. Climatic factors*

463 The low spatial resolution of the reanalysis data makes it difficult to ensure that the IDW-
464 interpolated air temperature/wind speed can represent the actual local situation for each single
465 lake. However, the large-scale spatial distribution of meteorological factors and the change rates
466 of the lakes over 17 years on the TP can be obtained from the data. In addition, available lake
467 water surface temperature (LWST) data for 57 lakes (except for Youbucuo Lake in the Inner II)
468 from 2002 to 2015 derived from MODIS Land Surface Temperature (LST) products by Wan et
469 al. (2017) are used.

470 Compared to the Inner II, the Inner I has a lower mean annual air temperature, LSWT and
471 wind speed from 2001 to 2017 (Table 4). Under relatively cold conditions with low wind speed,
472 lakes in the Inner I have earlier freeze-up dates, later break-up dates and longer ice cover
473 durations than do lakes in the Inner II. There are significant correlations between the ice
474 phenology parameters and climatic factors in the Inner basin, which can pass a two-tailed test

475 with a confidence level of 0.01 (Figure 8). It is probably because the climate factors differ with
476 different lake surroundings (latitude, altitude, etc.) naturally (Guo et al. 2018).

477 The mean air temperature, LSWT and wind speed for each of the study lakes are calculated.
478 For every 1°C increase in air temperature or LSWT or 1 m s⁻¹ increase in wind speed, the ice
479 cover duration is shortened by 13.75 days, 18.87 days and 29.81 days, respectively (Table 5).
480 LSWT has the highest correlation with lake ice phenology among the three climatic factors
481 (Figure 8, Table 5) (Bussieres et al., 2002). In addition, climate variability and changes have
482 greater effects on lake break-up dates than freeze-up dates (Figure 8, Table 5) (Palecki & Barry,
483 1986).

484 The energy available for water freeze-up in a lake is affected by the heat exchange with the
485 atmosphere, heat stored in the water body, and inflows of water (Williams, 1965). The heat
486 exchange with the atmosphere is mainly determined by climatic factors such as air/water
487 temperature, wind and solar radiation, while heat storage in a lake is determined additionally by
488 lake morphometry (Williams, 1965; Brown & Duguay, 2010), which will be discussed in the
489 next section. The ice break-up is affected by heat gain from the atmosphere, solar radiation, snow
490 and ice conditions, wind and currents, and inflows (Williams, 1965). Air and water temperature
491 directly drives the lake heat balance and thus plays the main role in the ice cover regime
492 (Kouraev et al., 2007), but the influence of wind is more complex. On the one hand, wind will
493 bring cold or warm currents, which affect the water surface temperature, and on the other hand,
494 the dynamic effects of wind could break the thin ice (Kouraev et al., 2007; Brown & Duguay,
495 2010). However, without detailed field observations, it is difficult to discuss the detailed effects
496 of these climatic factors on lake ice phenology on the TP lakes.

497 *5.2.2. Lake location, physico-chemical conditions and other factors*

498 To control the differences in climate conditions, the correlations between lake ice
499 phenology and lake altitude, area, and mineralization are calculated separately for the Inner I and
500 Inner II. Some of these lakes have no historical records of mineralization; thus, only the salt
501 lakes with mineralization data are used (Table 6).

502 There is a significant positive correlation between the altitudes and break-up end dates of
503 the lakes in the Inner basin. The higher the altitude, the later the break-up end date and the longer
504 the ice cover duration. There is an obvious autocorrelation between the altitude and climatic
505 conditions that together affect the break-up time of the lakes, while the freeze-up time is mainly
506 affected by the physical and chemical characteristics of the lakes (Adrian et al., 2009; Yao et al.,
507 2016).

508 Lakes with larger areas have more water-storage capacity and a stronger dynamic effect,
509 resulting in a longer freeze-up duration (Yao et al., 2016). Furthermore, wind can break up the
510 initial ice cover more easily (Kouraev et al., 2007; Brown & Duguay, 2010). Lakes with long
511 freeze-up durations in the Inner basin such as Qinghai Lake, Selin Co and Ngangla Ringco are
512 all lakes with areas larger than 500 km² (Table A1). In theory, lakes with higher mineralizations
513 should have a lower ice point, as well as a later freeze-up date, earlier break-up date and shorter
514 ice cover duration (Yao et al., 2016). Lakes, such as Selin Co, Nam Co, and Tu Co, with large
515 areas but low mineralization may affect the results of the correlation analysis (Table 6). In this
516 case, lake size has a greater impact on the ice phenology than does the mineralization. At the
517 same time, currently available mineralization records are from the 1970s to 1990s (Wang & Dou,
518 1998). In the context of climate change, the mineralization of lakes on the TP may have changed
519 greatly over the past several decades. For example, the reduction of lake water volume may lead

520 to an increase in mineralization and the expansion of the lake area may lead to a desalination of
521 water.

522 Lexiewudan Co, which has the highest change rate of ice phenology over the 17 years, had
523 a mineralization of 135.50 g L^{-1} in 1990 (Wang & Dou, 1998) and dropped to 89.47 g L^{-1} in 2010
524 (He et al., 2015). The lake came through an obvious process of desalination. Apart from this, the
525 lake is recharged with ice-snow meltwater and large amounts of spring water (Wang & Dou,
526 1998). The special recharge form may also be one of the reasons that caused the large change in
527 ice phenology. In addition, Dogaicoring Qangco may have similar reasons for the large changes
528 in recent years, as the lake is nearby Lexiewudan Co and has similar conditions as Lexiewudan
529 Co.

530 Shallow lakes require less heat to freeze-up and have earlier freeze-up dates (Kropacek et
531 al., 2013; Yao et al., 2016). The physical characteristics determine the thermodynamics of a lake
532 and sometimes have more of an impact on the ice phenology than do the chemical conditions.
533 For example, the weather conditions of Gahai and Qinghai Lake are similar, and the freeze-up
534 dates are nearly on the same day. As one of the remaining sub-lakes of Qinghai Lake, Gahai has
535 no surface inflow and a smaller area (Gahai: 44.68 km^2 , Qinghai Lake: $4,254.9 \text{ km}^2$, Wan et al.,
536 2014) as well as a shallower depth (Gahai: 8.0~9.5 m, Qinghai Lake: average of 17.9 m, Wang &
537 Dou, 1998). Although Gahai has a higher mineralization of 31.73 g L^{-1} than does Qinghai Lake
538 (13.84 g L^{-1}) (Wang & Dou, 1998), the mean freeze-up start date is 15 days earlier than that of
539 Qinghai Lake.

540 **6. Conclusions**

541 Approximately two-thirds of the cloud cover from the MODIS daily snow cover products
542 can be eliminated by gap filling approach combining Terra and Aqua data and using the pixels
543 within two days before and after the cloud covered pixel. The water cover classification from
544 cloud-removed MODIS data agree well with the Landsat data (28 scenes, MAE = 4.58%) for two
545 validated lakes (Nam Co and Selin Co) during the freeze-up and break-up periods. On this basis,
546 the freeze-up start and break-up end dates of the 58 lakes on the TP from 2001 to 2017 are
547 extracted. The freeze-up end and break-up start dates of 18 lakes were simultaneously extracted,
548 and the lake ice durations (including freeze-up duration, complete freezing duration, break-up
549 duration and ice cover duration) are calculated based on freeze-up/break-up dates. Compared to
550 freeze-up dates (MAEs range from 2.92 to 7.25 days), the break-up dates (MAEs range from
551 1.75 to 3.25 days) have a better consistent with different passive microwave data sets (derived
552 from AMSR-E/2 and SSM/I).

553 From late October to mid-January of the following year, the lakes on the TP begin to freeze
554 one after another (mainly from northern part to southern part). Over 17 years, the freeze-up start
555 dates of 81.03% of lakes have been delayed at a mean rate of 0.55 d yr^{-1} , and the other 18.97% of
556 lakes have advancing freeze-up start date at a mean change rate of 0.44 d yr^{-1} . From late March
557 to early July, the lakes gradually end their ice cover periods (mainly from southern part to
558 northern part). Over 17 years, the lakes whose break-up end dates have been delayed and
559 advanced account for 50% each, with mean change rates of 0.69 d yr^{-1} and 0.39 d yr^{-1} ,
560 respectively. The mean ice cover duration of 58 lakes is 157.78 days, of which the shortest is less
561 than three months, and the longest is eight months. From 2001 to 2017, there are 18 lakes with
562 ice cover durations that extended at a mean change rate of 1.11 d yr^{-1} , and 40 lakes shortened

563 their ice cover durations at a mean change rate of 0.80 d yr^{-1} . Furthermore, the freeze-up and
564 break-up processes of 18 lakes are extracted; the mean freeze-up duration is 9.81 days, the mean
565 break-up duration is 13.01 days, and the mean complete freezing duration is 121.12 days. Most
566 lakes have shorter freeze-up durations than break-up durations, and the freeze-up and break-up
567 rates of most lakes have increased over the 17 years.

568 The ice phenology is influenced by climatic conditions, geographical location, and the
569 physico-chemical characteristics of the lake. Lakes in the region with a lower altitude, higher
570 air/water temperature and higher wind speed are inclined to have later freeze-up and earlier
571 break-up dates, as well as shorter ice cover durations. The physico-chemical characteristics of
572 the lakes mainly affect the freeze-up dates; deeper lakes with larger areas and higher
573 mineralizations tend to have later freeze-up dates. Sometimes lake physical conditions may have
574 a greater impact on ice phenology than do the chemical conditions.

575 The lack of historical observational data makes it difficult to study lake ice phenology on
576 the TP without using remote sensing data. The quality of MODIS daily snow cover products
577 limits the number of lakes that can be studied, and the low spatial resolution of reanalysis data
578 makes it difficult to represent the actual meteorological conditions of each lake. It is also difficult
579 to ensure the reliability of historical lake physico-chemical data that were collected several
580 decades ago. With the improvement of data and methods, lake ice phenology on the TP and its
581 influencing factors can hopefully be further analyzed in the future. In addition, further research is
582 required on the comparisons of lake ice phenology characteristics derived from different sources
583 of remote sensing data and different retrieval methods, as well as in different climatic regions.

584 **Acknowledgments**

585 This work is supported financially by the Program for National Natural Science Foundation of China
586 (No. 41830105) and also funded by the International Scholar Exchange Fellowship (ISEF) program at
587 KFAS (Korean Foundation of Advanced Studies). The MODIS snow data used in this study are obtained
588 from the National Snow and Ice Data Center (<http://nsidc.org>). The Landsat data used are obtained from
589 the Google Earth Engine platform (<https://earthengine.google.com/>). The Reanalysis data are from the
590 National Oceanic and Atmospheric Administration (<https://www.esrl.noaa.gov/>). We would thank the two
591 anonymous reviewers and editors for valuable comments and suggestions to greatly improve the paper.

592 **References**

- 593 Adrian, R., O'Reilly, C. M., Zagarese, H., Baines, S. B., Hessen, D. O., Keller, W., et al. (2009).
594 Lakes as sentinels of climate change. *Limnology and Oceanography*, 54(6), 2283-2297.
595 http://dx.doi.org/10.4319/lo.2009.54.6_part_2.2283.
- 596 Brown, L. C. & Duguay, C. R. (2010). The response and role of ice cover in lake-climate
597 interactions. *Progress in Physical Geography*, 34, 671-704.
598 <http://dx.doi.org/10.1177/0309133310375653>.
- 599 Bussieres, N., Versegny, D. & MacPherson, J. I. (2002). The evolution of AVHRR-derived water
600 temperatures over boreal lakes. *Remote sensing of environment*, 80(3), 373-384.
601 [https://doi.org/10.1016/S0034-4257\(01\)00317-0](https://doi.org/10.1016/S0034-4257(01)00317-0).
- 602 Cai, Y., Ke, C. Q. & Duan, Z. (2017). Monitoring ice variations in Qinghai Lake from 1979 to
603 2016 using passive microwave remote sensing data. *Science of the Total Environment*, 607-608,
604 120-131. <http://dx.doi.org/10.1016/j.scitotenv.2017.07.027>.

- 605 Chaouch, N., Temimi, M., Romanov, P., Cabrera, R., McKillop, G. & Khanbilvardi, R. (2014).
606 An automated algorithm for river ice monitoring over the Susquehanna River using the MODIS
607 data. *Hydrological Processes*, 28(1), 62-73. <http://dx.doi.org/10.1002/hyp.9548>.
- 608 Che, T., Li, X. & Jin, R. (2009). Monitoring the frozen duration of Qinghai Lake using satellite
609 passive microwave remote sensing low frequency data (in Chinese). *Chinese Science Bulletin*,
610 54(6), 787-791. <http://dx.doi.org/10.1007/s11434-009-0044-3>.
- 611 Dörnhöfer, K. & Oppelt, N. (2016). Remote sensing for lake research and monitoring-Recent
612 advances. *Ecological Indicators*, 64, 105-122. <http://dx.doi.org/10.1016/j.ecolind.2015.12.009>.
- 613 Du, J. Y., Kimball, J. S., Duguay, C., Kin, Y. & Watts, J. D. (2017). Satellite microwave
614 assessment of Northern Hemisphere lake ice phenology from 2002 to 2015. *The Cryosphere*, 11,
615 47-63. <http://dx.doi.org/10.5194/tc-2016-199>.
- 616 Duguay, C. R., Bernier, M., Gauthier, Y. & Kouraev, A. (2015). Remote sensing of lake and
617 river ice. In M. Tedesco (Ed.) *Remote Sensing of the Cryosphere* (pp. 273-306). Oxford, UK:
618 Wiley-Blackwell. <http://dx.doi.org/10.1002/9781118368909.ch12>.
- 619 Duguay, C. R. & Lafleur, P. M. (2003). Estimating depth and ice thickness of shallow subarctic
620 lakes using spaceborne optical and SAR data. *International Journal of Remote Sensing*, 24(3),
621 475–489. <http://dx.doi.org/10.1080/01431160304992>.
- 622 Duguay, C. R., Pultz, T. J., Lafleur, P. M. & Drai, D. (2002). RADARSAT backscatter
623 characteristics of ice growing on shallow sub-arctic lakes, Churchill, Manitoba, Canada.
624 *Hydrological Processes*, 16(8), 1631–1644. <http://dx.doi.org/10.1002/hyp.1026>.

- 625 Gafurov, A. & Bárdossy, A. (2009). Cloud removal methodology from MODIS snow cover
626 product. *Hydrology and Earth System Sciences*, 13(7), 1361-1373.
627 <http://dx.doi.org/10.5194/hess-13-1361-2009>.
- 628 Gao, Y., Xie, H. J., Lu, N., Yao, T. D. & Liang, T. G. (2010). Toward advanced daily cloud-free
629 snow cover and snow water equivalent products from Terra–Aqua MODIS and Aqua AMSR-E
630 measurements. *Journal of Hydrology*, 385(1-4), 23-35.
631 <https://doi.org/10.1016/j.jhydrol.2010.01.022>.
- 632 Gao, Y., Xie, H. J., Yao, T. D. & Xue, C. S. (2010). Integrated assessment on multi-temporal and
633 multi-sensor combinations for reducing cloud obscuration of MODIS snow cover products of the
634 Pacific Northwest USA. *Remote Sensing of Environment*, 114(8), 1662-1675.
635 <https://doi.org/10.1016/j.rse.2010.02.017>.
- 636 Geldsetzer, T., Sanden, J. V. D. & Brisco, B. (2010). Monitoring lake ice during spring melt
637 using RADARSAT-2 SAR. *Canadian Journal of Remote Sensing*, 36(S2), S391-S400.
- 638 Guo, L. N., Wu, Y. H., Zheng, H. X., Zhang, B., Li, J. S., Zhang, F. F. & Shen, Q. (2018).
639 Uncertainty and variation of remotely sensed lake ice phenology across the Tibetan Plateau.
640 *Remote Sensing*, 10, 1534. <https://doi.org/10.3390/rs10101534>.
- 641 Hall, D. K. & Riggs, G. A. (2007). Accuracy assessment of the MODIS snow products.
642 *Hydrological Processes*, 21(12), 1534-1547. <http://dx.doi.org/10.1002/hyp.6715>.
- 643 Hall, D. K., Riggs, G. A. & Salomonson, V. V. (2001). Algorithm Theoretical Basis Document
644 (ATBD) for the MODIS Snow and Sea Ice-Mapping Algorithms. [https://modis-snow-
645 ice.gsfc.nasa.gov/?c=atbd&t=atbd](https://modis-snow-ice.gsfc.nasa.gov/?c=atbd&t=atbd).

- 646 He, L., Han, F. Q., Han, W. X., Yan, J. P., Li, B. K., Han, Y. Z., et al. (2015). Hydrochemical
647 Characteristics of Lexiewudan Lake in Hoh Xil, Qinghai (in Chinese). *Journal of Salt Lake*
648 *Research*, 23(2), 28-33.
- 649 Howell, S. E. L., Brown, L. C., Kang, K. -K. & Duguay, C. R. (2009). Variability in ice
650 phenology on Great Bear Lake and Great Slave Lake, Northwest Territories, Canada, from
651 SeaWinds/QuikSCAT: 2000-2006. *Remote Sensing of Environment*, 113(4), 816-834.
652 <http://dx.doi.org/10.1016/j.rse.2008.12.007>.
- 653 Huang, H., Liang, T., Zhang, X. & Guo, Z. (2011). Validation of MODIS snow cover products
654 using Landsat and ground measurements during the 2001-2005 snow seasons over northern
655 Xinjiang, China. *International Journal of Remote Sensing*, 32(1), 133-152.
656 <http://dx.doi.org/10.1080/01431160903439924>.
- 657 Jeffries, M. O., Morris, K., Weeks, W. F. & Wakabayashi, H. (1994). Structural and stratigraphic
658 features and ERS 1 synthetic aperture radar backscatter characteristics of ice growing on shallow
659 lakes in NW Alaska, winter 1991–1992. *Journal of Geophysical Research Oceans*, 99(C11),
660 22459–22471. <http://dx.doi.org/10.1029/94JC01479>.
- 661 Kang, S. C., Xu, Y. W., You, Q. L., Flügel, W. -A., Pepin, N. & Yao, T. D. (2010). Review of
662 climate and cryospheric change in the Tibetan Plateau. *Environmental Research Letters*, 5,
663 015101. <http://dx.doi.org/10.1088/1748-9326/5/1/015101>.
- 664 Ke, C. Q., Tao, A. Q. & Jin, X. (2013). Variability in the ice phenology of Nam Co Lake in
665 central Tibet from scanning multichannel microwave radiometer and special sensor
666 microwave/imager: 1978 to 2013. *Journal of Applied Remote Sensing*, 7, 073477.
667 <http://dx.doi.org/10.1117/1.JRS.7.073477>.

- 668 Kendall, M. G. (1975). *Rank Correlation Methods*. London: Charles Griffin.
- 669 Kouraev, A. V., Semovski, S. V., Shimaraev, M. N., Mognard, N. M., Legrésy, B & Rémy, F.
670 (2007). The ice regime of Lake Baikal from historical and satellite data: Relationship to air
671 temperature, dynamical, and other factors. *Limnology and Oceanography*, 52(3), 1268-1286.
672 <http://dx.doi.org/10.4319/lo.2007.52.3.1268>.
- 673 Kropáček, J., Maussion, F., Chen, F., Hoerz, S. & Hochschild, V. (2013). Analysis of ice
674 phenology of lakes on the Tibetan Plateau from MODIS data. *The Cryosphere*, 7(1), 287-301.
675 <http://dx.doi.org/10.5194/tc-7-287-2013>.
- 676 Latifovic, R. & Pouliot, D. (2007). Analysis of climate change impacts on lake ice phenology in
677 Canada using the historical satellite data record. *Remote Sensing of Environment*, 106(4), 492-
678 507. <http://dx.doi.org/10.1016/j.rse.2006.09.015>.
- 679 Liang, T. G., Zhang, X. T., Xie, H. J., Wu, C. X., Feng, Q. S., Huang, X. D. & Chen, Q. G.
680 (2008). Toward improved daily snow cover mapping with advanced combination of MODIS and
681 AMSR-E measurements. *Remote Sensing of Environment*, 112(10), 3750-3761.
682 <https://doi.org/10.1016/j.rse.2008.05.010>.
- 683 Liu, X. D. & Chen, B. D. (2000). Climatic warming in the Tibetan Plateau during recent decades.
684 *International Journal of Climatology*, 20, 1729-1742. [http://dx.doi.org/10.1002/1097-0088\(20001130\)20:14<1729::AID-JOC556>3.0.CO;2-Y](http://dx.doi.org/10.1002/1097-0088(20001130)20:14<1729::AID-JOC556>3.0.CO;2-Y).
- 685
- 686 López-Burgos, V., Gupta, H. V. & Clark, M. (2013). Reducing cloud obscuration of MODIS
687 snow cover area products by combining spatio-temporal techniques with a probability of snow
688 approach. *Hydrology and Earth System Sciences*, 17(5), 1809-1823.
689 <http://dx.doi.org/10.5194/hess-17-1809-2013>.

- 690 Mann, H. B. (1945). Non-parametric tests against trend. *Econometrica*, 13, 245-259.
691 <http://dx.doi.org/10.2307/1907187>.
- 692 Maurer, E. P., Rhoads, J. D., Dubayah, R. O. & Lettenmaier, D. P. (2003). Evaluation of the
693 snow-covered area data product from MODIS. *Hydrological Processes*, 17, 59-71.
694 <http://dx.doi.org/10.1002/hyp.1193>.
- 695 Morris, K., Jeffries, M. O. & Weeks, W. F. (1995). Ice processes and growth history on Arctic
696 and sub-Arctic lakes using ERS-1 SAR data. *Polar Record*, 31(177), 115–128.
697 <http://dx.doi.org/10.1017/S0032247400013619>.
- 698 Palecki, M. A. & Barry, R. G. (1986). Freeze-up and break-up of lakes as an index of
699 temperature changes during the transition seasons: a case study for Finland. *Journal of Climate*
700 *and Applied Climatology*, 25, 893-902. [https://doi.org/10.1175/1520-](https://doi.org/10.1175/1520-0450(1986)025<0893:FUABUO>2.0.CO;2)
701 [0450\(1986\)025<0893:FUABUO>2.0.CO;2](https://doi.org/10.1175/1520-0450(1986)025<0893:FUABUO>2.0.CO;2).
- 702 Parajka, J. & Blöschl, G. (2008). The value of MODIS snow cover data in validating and
703 calibrating conceptual hydrologic models. *Journal of Hydrology*, 358(3-4), 240-258.
704 <http://dx.doi.org/10.1016/j.jhydrol.2008.06.006>.
- 705 Paudel, K. P. & Andersen, P. (2011). Monitoring snow cover variability in an agropastoral area
706 in the Trans Himalayan region of Nepal using MODIS data with improved cloud removal
707 methodology. *Remote Sensing of Environment*, 115(5), 1234-1246.
708 <http://dx.doi.org/10.1016/j.rse.2011.01.006>.
- 709 Qiu, J. (2008). The Third Pole. *Nature*, 454(7203), 393-396. <http://dx.doi.org/10.1038/454393a>.

- 710 Reed, B., Buddle, M., Spencer, P. & Miller, A. E. (2009). Integration of MODIS-derived metrics
711 to assess interannual variability in snowpack, lake ice, and NDVI in southwest Alaska. *Remote*
712 *Sensing of Environment*, 113(7), 1443-1452. <http://dx.doi.org/10.1016/j.rse.2008.07.020>.
- 713 Rouse, W. R., Oswald, C. J., Binyamin, J., Spence, C., Schertzer, W. M., Blanken, P. D., et al.
714 (2005). The Role of Northern Lakes in a Regional Energy Balance. *Journal of*
715 *Hydrometeorology*, 6, 291-305. <https://doi.org/10.1175/JHM421.1>.
- 716 Sorman, A. U., Akyurek, Z., Sensoy, A., Sorman, A. A. & Tekeli, A. E. (2007). Commentary on
717 comparison of MODIS snow cover and albedo products with ground observations over the
718 mountainous terrain of Turkey. *Hydrology and Earth System Sciences*, 11(4), 1353-1360.
719 <http://dx.doi.org/10.5194/hess-11-1353-2007>.
- 720 Wan, W., Li, H., Xie, H. J., Hong, Y., Long, D., Zhao, L. M., et al. (2017). A comprehensive
721 data set of lake surface water temperature over the Tibetan Plateau derived from MODIS LST
722 products 2001–2015. *Scientific Data*, 4, 170095. <http://dx.doi.org/10.1038/sdata.2017.95>.
- 723 Wan, W., Xiao, P. F., Feng, X. Z., Li, H., Ma, R. H., Duan, H. T. & Zhao, L. M. (2014).
724 Monitoring lake changes of Qinghai-Tibetan Plateau over the past 30 years using satellite remote
725 sensing data. *Chinese Science Bulletin*, 59(10), 1021-1035. [http://dx.doi.org/10.1007/s11434-](http://dx.doi.org/10.1007/s11434-014-0128-6)
726 [014-0128-6](http://dx.doi.org/10.1007/s11434-014-0128-6).
- 727 Wang, S. M. & Dou, H. S. (1998). *Records of Chinese Lakes* (in Chinese). Beijing, CHN:
728 Science Press.
- 729 Weber, H., Riffler, M., Nöges, T. & Wunderle, S. (2016). Lake ice phenology from AVHRR
730 data for European lakes: An automated two-step extraction method. *Remote Sensing of*
731 *Environment*, 174, 329-340. <http://dx.doi.org/10.1016/j.rse.2015.12.014>.

- 732 Wei, Q. F. & Ye, Q. H. (2010). Review of lake ice monitoring by remote sensing (in Chinese).
733 *Progress in Geography*, 29(7), 803–810.
- 734 Williams, G. P. (1965). Correlating freeze-up and break-up with weather conditions. *Canadian*
735 *Geotechnical Journal*, 11(4), 313-326. <http://doi.org/10.1139/t65-047>.
- 736 Yao, X. J., Li, L., Zhao, J., Sun, M. P., Li, J., Gong, P. & An, L. N. (2016). Spatial-temporal
737 variations of lake ice phenology in the Hoh Xil region from 2000 to 2011. *Journal of*
738 *Geographical Sciences*, 26(1), 70-82. <http://dx.doi.org/10.1007/s11442-016-1255-6>.
- 739 Yu, J. Y., Zhang, G. Q., Yao, T. D., Xie, H. J., Zhang, H. B., Ke, C. Q. & Yao, R. Z. (2016).
740 Developing Daily Cloud-Free Snow Composite Products from MODIS Terra–Aqua and IMS for
741 the Tibetan Plateau. *IEEE Transactions on Geoscience & Remote Sensing*, 54(4), 2171-2180.
742 <http://doi.org/10.1109/TGRS.2015.2496950>.
- 743 Zhang, G. Q., Yao, T. D., Xie, H. J., Kang, S. C. & Lei, Y. B. (2013). Increased mass over the
744 Tibetan Plateau: From lakes or glaciers? *Geophysical Research Letters*, 40(10), 2125-2130.
745 <http://dx.doi.org/10.1002/grl.50462>.
- 746 Zhang, G. Q., Yao, T. D., Xie, H. J., Qin, J., Ye, Q. H., Dai, Y. F. & Guo, R. F. (2014).
747 Estimating surface temperature changes of lakes in the Tibetan Plateau using MODIS LST data.
748 *Journal of Geophysical Research Atmospheres*, 119(14), 8552–8567.
749 <http://dx.doi.org/10.1002/2014JD021615>.
- 750 Zhang, G. Q., Yao, T. D., Xie, H. J., Zhang, K. X. & Zhu, F. J. (2014). Lakes' state and
751 abundance across the Tibetan Plateau. *Chinese Science Bulletin*, 59(24), 3010-3021.
752 <http://dx.doi.org/10.1007/s11434-014-0258-x>.
- 753

754

755

756

757

758

759

760

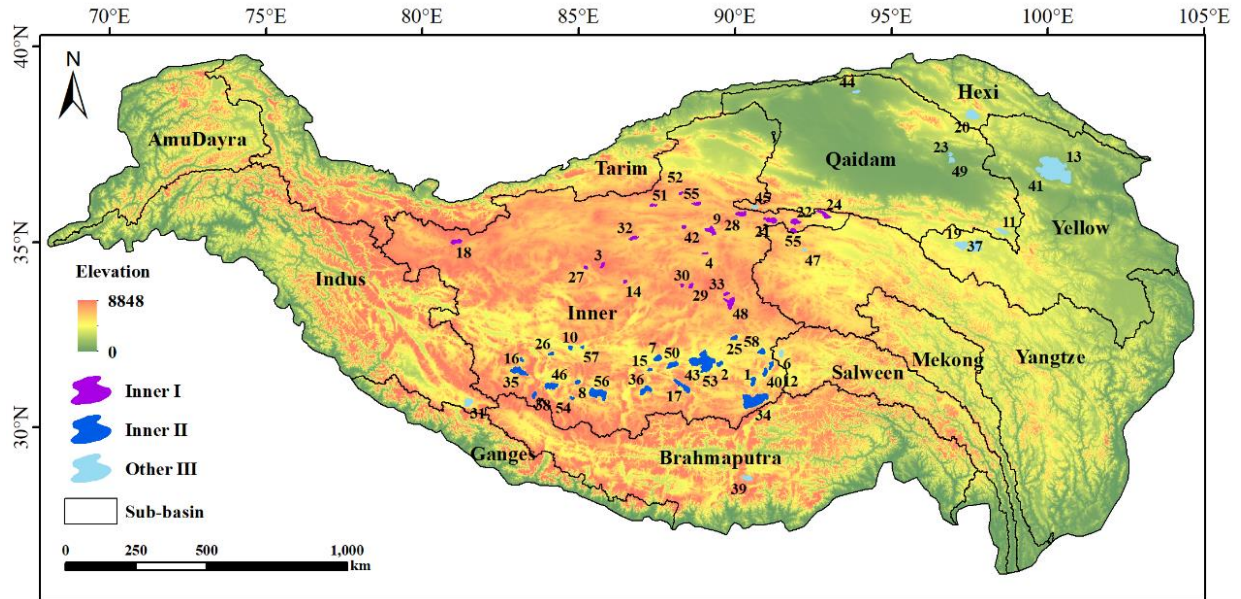
761

762

763

764

765 **Figure Captions**



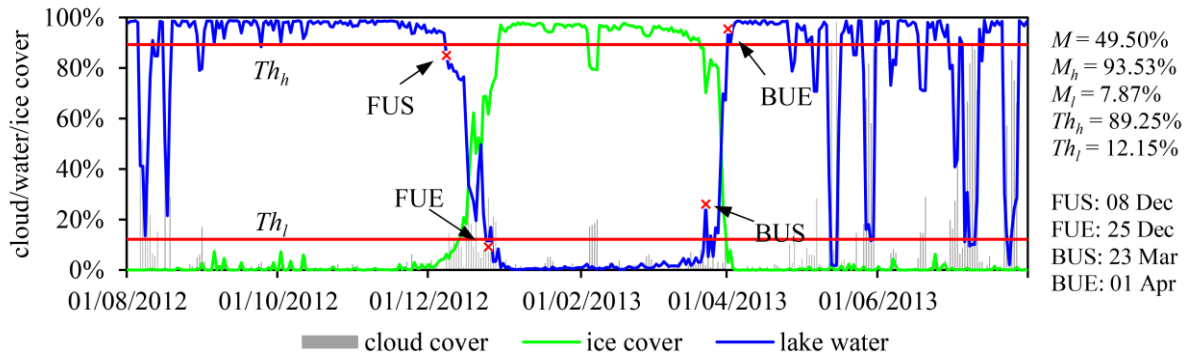
766

767 **Figure 1.** Locations of the TP and its sub-basins. 58 study lakes are grouped into three sub-areas
 768 labeled Inner I, Inner II, and Other III (The lake names are listed in Table A1 in Appendix A).

769

770

771



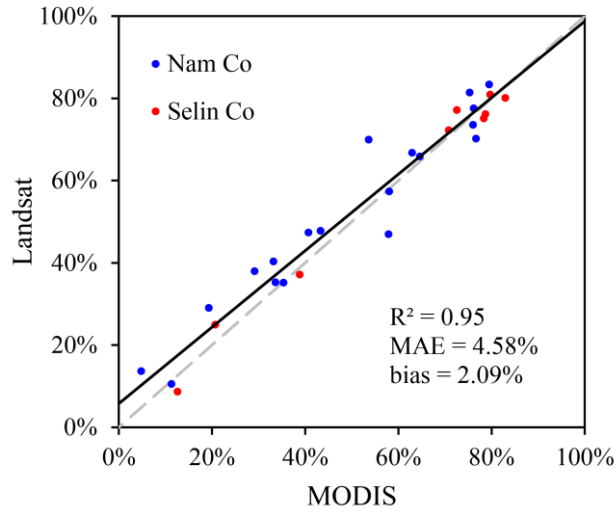
772

773 **Figure 2.** The extraction of the freeze-up/break-up dates in Qinghai Lake during 2013. Two red
 774 lines represent the two thresholds for extracting freeze-up/break-up dates, and four red stars,
 775 from left to right, represent the freeze-up start (FUS), freeze-up end (FUE), break-up start (BUS),
 776 and break-up end (BUE) dates.

777

778

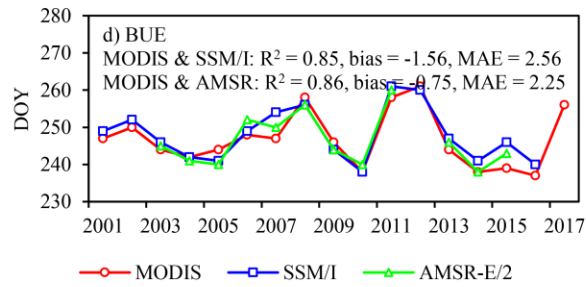
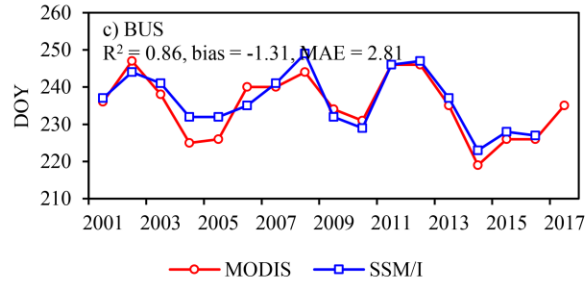
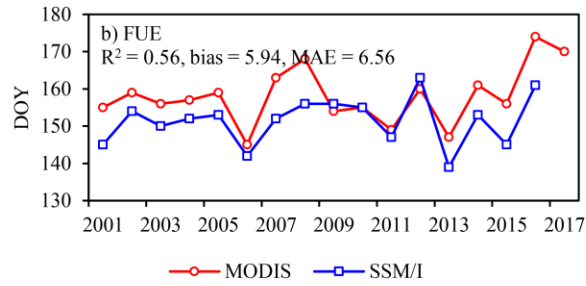
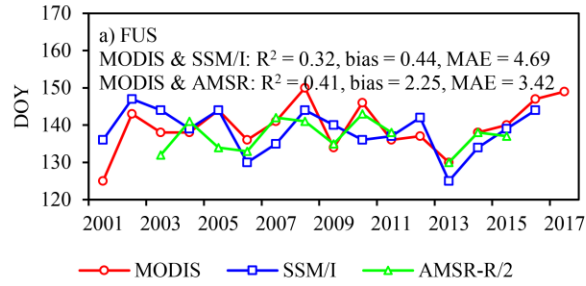
779



780

781 **Figure 3.** Comparison of lake water cover proportions during freeze-up/break-up periods derived
782 from the MODIS cloud-removed data and Landsat data.

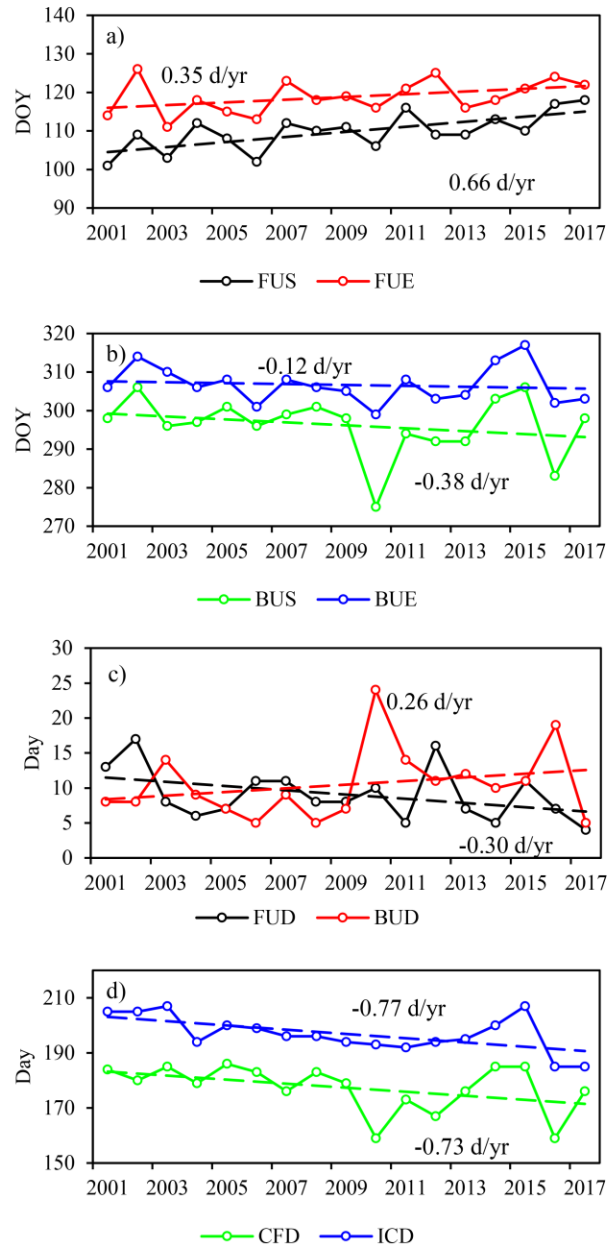
783



784

785 **Figure 4.** Comparisons of ice phenology for Qinghai Lake derived from MODIS data and
786 passive microwave data. **a.** Comparisons between freeze-up start (FUS) dates derived from
787 MODIS, SSM/I and AMSR; **b.** comparisons between freeze-up end (FUE) dates derived from
788 MODIS and SSM/I; **c.** comparisons between break-up start (BUS) dates derived from MODIS
789 and SSM/I; and **d.** comparisons between break-up end (BUE) dates derived from MODIS, SSM/I
790 and AMSR. DOY means the day of the year relative to 1 August.

791



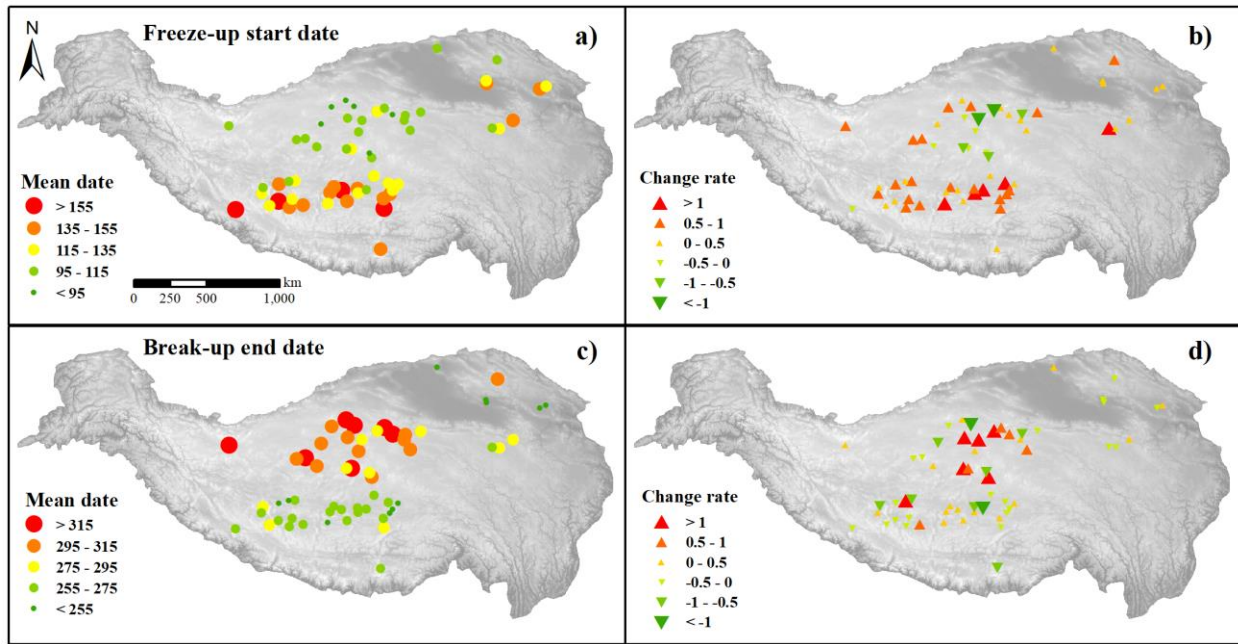
792

793 **Figure 5.** The ice phenology and its trend for Har Lake from 2001 to 2017. **a.** Freeze-up dates
 794 and their trends; **b.** break-up dates and their trends; **c.** freeze-up duration and break-up duration
 795 and their trends; and **d.** complete freezing durations and ice cover duration and their trends over
 796 17 years. (FUS: freeze-up start, FUE: freeze-up end, BUS: break-up start, BUE: break-up end,

797 FUD: freeze-up duration, BUD: break-up duration, CFD: complete freezing duration, and ICD:
 798 ice cover duration)

799

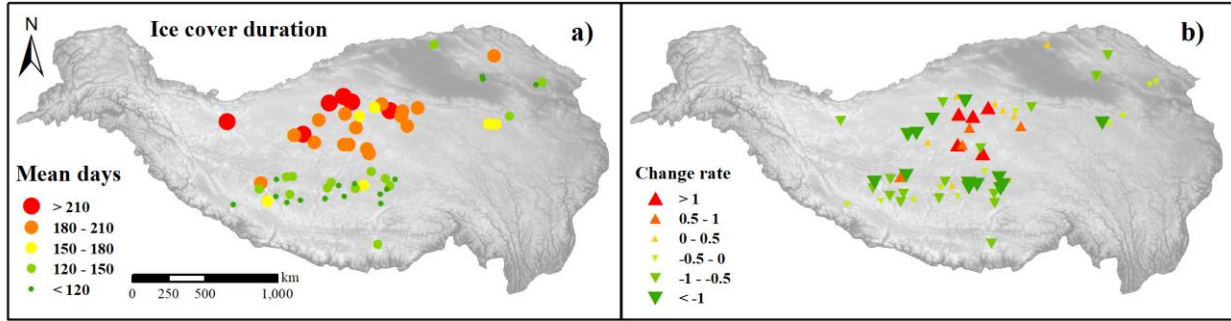
800



801

802 **Figure 6.** Mean and change rate (d yr^{-1}) of freeze-up start and break-up end dates of the 58 lakes
 803 from 2001 to 2017. **a.** Mean freeze-up start date; **b.** change rate of freeze-up start date; **c.** the
 804 mean break-up end date; and **d.** change rate of break-up end date. (The freeze-up/break-up dates
 805 are DOYs.)

806



807

808 **Figure 7.** Mean and change rate of ice cover duration for the 58 lakes from 2001 to 2017. **a.**
809 Mean ice cover duration; and **b.** change rate of ice cover duration.

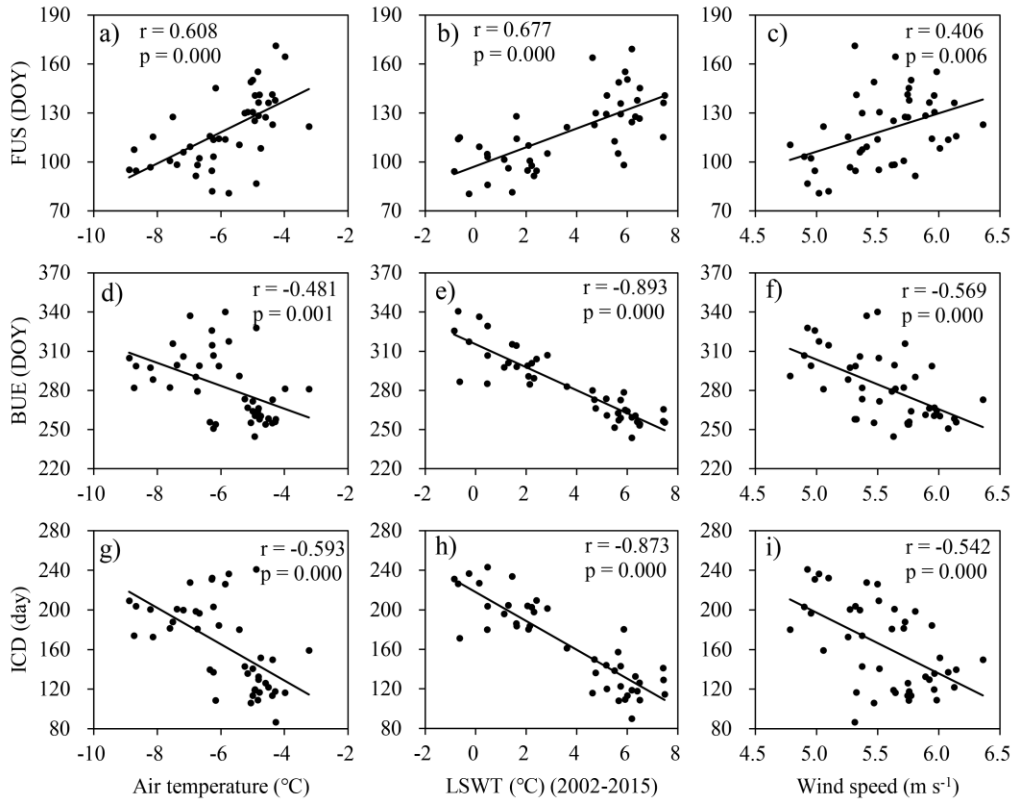
810

811

812

813

814



815

816 **Figure 8.** Correlations between mean air temperature, LSWT (lake water surface temperature),
 817 wind speed and mean lake ice phenology parameters in the Inner basin from 2001 to 2017. (FUS:
 818 freeze-up start, BUE: break-up end and ICD: ice cover duration)

819

820

821

822

823

824

825 **Table Captions**

826 **Table 1.** *Comparison of Cloud Cover for 58 Lakes During 2013, With and Without Cloud*
 827 *Removal*

	Mean	Maximum	Minimum
Original Terra	44.97%	63.98% (Taiyang Lake)	30.07% (Zhaxi Co)
Original Aqua	51.70%	69.43% (Taiyang Lake)	31.47% (Mapam Yumco)
Combined T&A	31.02%	50.94% (Taiyang Lake)	18.58% (Lagkor Co)
Cloud removal	16.54%	35.49% (Taiyang Lake)	4.52% (Zhari Namco)

828 **Table 2.** *Summary of the Comparison Results for Freeze-up Start (FUS) and Break-up End*
 829 *(BUE) Dates Derived From MODIS Snow Products, AMSR-E/2 Data Sets and SSM/I Data Sets*

		FUS			BUE		
	Lake	R ²	bias	MAE	R ²	bias	MAE
MODIS compared against AMSR-E/2	Gyaring Lake	0.09	0.50	5.33	0.97	0.67	2.50
	Har Lake	0.62	-0.58	2.92	0.84	-0.83	2.17
	Nam Co	0.19	3.58	7.08	0.79	0.75	3.25
	Ngangla Ringco	0.28	-4.33	5.83	0.91	-0.17	1.83
	Ngoring Lake	0.19	0.83	6.83	0.93	-0.58	2.25
	Qinghai Lake	0.41	2.25	3.42	0.86	-0.75	2.25
	Selin Co	0.48	-7.25	7.25	0.93	0.75	1.75
	Zhari Namco	0.54	-2.83	3.83	0.96	-1.50	2.00
	Average	0.35	-0.98	5.31	0.90	-0.21	2.25
MODIS compared against SSM/I	Nam Co	0.42	-5.38	6.92	0.35	0.00	6.31
	Qinghai Lake	0.32	0.44	4.69	0.85	-1.56	2.56
	Average	0.37	-2.47	5.81	0.60	-0.78	4.44

830

831

832 **Table 3.** *The Number and Percentage of Lakes, Their Mean Date/Days and Change Rates ($d yr^{-1}$)*
 833 *Within Three Sub-areas: Inner I, Inner II and Other III (FUS: Freeze-up Start, BUE: Break-up*
 834 *End, and ICD: Ice Cover Duration)*

		Inner I	Inner II	Other III	All lakes
FUS	Mean (all)	20 (34.48%), 10 Nov	24 (41.38%), 13 Dec	14 (24.14%), 5 Dec	58 (100%), 30 Nov
	Delaying	10 (50.00%), 0.57	24 (100.00%), 0.64	13 (92.86%), 0.35	47 (81.03%), 0.55
	Advancing	10 (50.00%), -0.49	0	1 (7.14%), -0.00	11 (18.97%), -0.44
BUE	Mean (all)	3 Jun	20 Apr	26 Apr	6 May
	Delaying	12 (60.00%), 1.21	11 (45.83%), 0.32	6 (42.86%), 0.35	29 (50.00%), 0.69
	Advancing	8 (40.00%), -0.51	13 (54.17%), -0.44	8 (57.14%), -0.19	29 (50.00%), -0.39
ICD	Mean (all)	204.46	128.21	141.79	157.78
	Extending	11 (55.00%), 1.62	3 (12.50%), 0.41	4 (28.57%), 0.24	18 (31.03%), 1.11
	Shortening	9 (45.00%), -0.92	21 (87.50%), -0.89	10 (71.43%), -0.50	40 (68.97%), -0.80

835

836

837 **Table 4.** *Comparison of Climate Conditions Between the Inner I and Inner II From 2001 to 2017*
 838 *(CR: Change Rates, LSWT: Lake Water Surface Temperature)*

	Air temperature		LSWT (2002-2015)		Wind speed	
	Mean ($^{\circ}C$)	CR ($0.01^{\circ}C yr^{-1}$)	Mean ($^{\circ}C$)	CR ($0.01^{\circ}C yr^{-1}$)	Mean ($m s^{-1}$)	CR ($0.01 m s^{-1} yr^{-1}$)
Inner I	-6.98	4.30	1.10	-5.26	5.32	1.07
Inner II	-4.94	6.89	5.48	-1.47	5.76	2.31

839

840

841 **Table 5.** *The Number of Lakes Whose Ice Phenology Has a Significant Correlation ($p < 0.05$)*
 842 *With Climatic Factors, and the Mean Change Rates (FUS: Freeze-up Start, BUE: Break-up End,*
 843 *and ICD: Ice Cover Duration, LSWT: Lake Water Surface Temperature)*

	Air temperature (d °C ⁻¹)	LSWT (d °C ⁻¹)	Wind speed (d m ⁻¹ s)
FUS	7, 8.53	9, 2.55	7, 13.89
BUE	10, -11.11	30, -14.56	11, -26.83
ICD	17, -13.75	23, -18.87	16, -29.81

844

845 **Table 6.** *Correlations Between Ice Phenology and the Physical Attributes of the Lakes in the*
 846 *Inner I and Inner II (FUS: Freeze-up Start, BUE: Break-up End, and ICD: Ice Cover Duration)*

	Inner I			Inner II		
	Altitude	Area	Mineralization ^a	Altitude	Area	Mineralization ^b
FUS	0.24	0.44	-0.04	-0.03	0.48*	-0.17
BUE	0.52*	-0.03	-0.28	0.65**	0.18	-0.03
ICD	0.28	-0.26	-0.24	0.34	-0.32	0.15

847 *Note.* ^a Calculated from eleven salt lakes. ^b Calculated from 19 salt lakes, and mineralization data
 848 are from Wang and Dou (1998). * Statistical significance at the 0.05 level. ** Statistical
 849 significance at the 0.01 level.

850

851 **Appendix A**

852 **Table A1.** *Lake Ice Phenology Statistics and the Change Rates (CR, d yr⁻¹) and Lake*
 853 *Characteristics for 58 Lakes From 2001 to 2017 (FUS: Freeze-up Start, FUE: Freeze-up End,*
 854 *BUS: Break-up Start, BUE: Break-up End, FUD: Freeze-up Duration, BUD: Break-up Duration,*
 855 *CFD: Complete Freezing Duration, and ICD: Ice Cover Duration)*

No.	Lake	Area (km ²) ^a	Altitude (m) ^b	Mean FUS	CR	Mean FUE	CR	Mean BUS	CR	Mean BUE	CR	Mean FUD	CR	Mean CFD	CR	Mean BUD	CR	Mean ICD	CR	Spatial location
1	Bamco	236.16	4560	16 Dec	0.82 [*]					13 Apr	0.25							117.88	-0.56	I
2	Bangkog Co	136.34	4527	17 Nov	1.10 [*]					18 Apr	-1.63 ^{**}							151.82	-2.73 ^{**}	I
3	Burog Co	89.91	5166	18 Nov	0.88 ^{**}					4 Jul	-0.39							227.82	-1.26	I
4	Changhu Lake	49.98	4839	4 Nov	-0.24					1 Jun	0.28							209.29	0.52	I
5	Cuoda Rima	84.6	4783	11 Nov	0.13					26 May	0.42							196.59	0.29	III
6	Cuona Lake	188.54	4585	3 Dec	0.19					25 Mar	0.36							112.06	0.16	I
7	Dagze Co	269.07	4465	15 Dec	0.79 ^{**}	20 Dec	0.63 [*]	2 Apr	0.82	16 Apr	0.20	5.18	-0.16	103.59	0.19	13.35	-0.63 ^{**}	122.12	-0.59	I
8	Dawa Co	110.55	4623	9 Dec	0.85 [*]	14 Dec	0.71 [*]	12 Apr	0.07	29 Apr	0.00	4.94	-0.14	118.65	-0.64 [*]	17.29	-0.07	140.88	-0.85	I
9	Dogaicoring Qangco	313.68	4787	16 Nov	-1.12					9 May	3.50 [*]							174.24	4.62	I
10	Dong Co	92.47	4394	22 Nov	0.27	28 Nov	0.20	1 Apr	1.10	8 Apr	1.02	6.18	-0.07	123.65	0.90	7.29	-0.08	137.12	0.75	I
11	Donggei Cuona Lake	230.65	4081	15 Dec	0.23 [*]					10 May	0.21							145.53	-0.02	III
12	Dung Co	149.6	4551	6 Dec	0.77 ^{**}					11 Apr	-0.35							126.29	-1.12	I
13	Gahai	44.68	3197	3 Dec	0.38					4 Apr	0.01							121.29	-0.37	III
14	Garkung Caka	59.33	4909	7 Nov	-0.04					27 May	0.13							200.82	0.17	I
15	Gemang Co	60.06	4605	15 Dec	0.35					24 Apr	0.05							129.76	-0.30	I
16	Gopug Co	59.68	4718	7 Nov	0.15					7 May	-0.88							181.00	-1.03	I
17	Goren Co	477.98	4649	29 Dec	0.25					21 Apr	0.25							113.59	0.00	I
18	Gozha Co	315.51	5080	22 Nov	0.67 ^{**}					7 Jul	0.03							226.12	-0.64	II
19	Gyaring Lake	526.62	4290	16 Nov	1.02 [*]					18 Apr	-0.27							153.12	-1.29	IV
20	Har Lake	596.39	4076	18 Nov	0.66 ^{**}	27 Nov	0.35	24 May	-0.38	3 Jun	-0.12	9.06	-0.30	177.35	-0.73 [*]	10.47	0.26	196.88	-0.77 [*]	III
21	Hoh Xil Lake	315.95	4886	3 Nov	0.47	15 Nov	0.15	12 Jun	0.93 [*]	22 Jun	0.58	11.47	-0.33	209.65	0.79	9.88 [*]	-0.35	231.00	0.11	III

22	Huolunuo'er	259.24	4753	12 Nov	-0.64				3 Jun	-0.65									203.35	-0.01	III
23	Keluke Lake	54	2814	27 Nov	0.14				27 Mar	-0.40									119.35	-0.54	III
24	Kusai Lake	271.08	4475	19 Nov	0.80**	4 Dec	0.51 [†]	6 May	0.09	18 May	-0.10	14.65	-0.28	153.71	-0.42	11.94	-0.19	180.29	-0.90 [°]	III	
25	Kyebxang Co	170.98	4615	1 Dec	0.48	9 Dec	0.42 [†]	17 Apr	0.51	30 Apr	-0.01	7.59	-0.06	128.71	0.10	13.65	-0.52	149.94	-0.48	I	
26	Lagkor Co	93.39	4467	24 Dec	0.80**	28 Dec	0.86**	30 Mar	-0.27	11 Apr	0.00	3.94	0.06	92.65	-1.13 [†]	12.00	0.26	108.59	-0.81	I	
27	Laxiong Co	60.75	4885	15 Nov	0.62**					2 Jun	-0.38								199.88	-1.01	I
28	Lexiewudan Co	247.58	4870	24 Nov	-1.22**					16 May	4.25**								172.76	5.46**	III
29	Lingguo Co	108.14	5062	6 Dec	-0.19					12 Jun	0.63								188.06	0.82	I
30	Longwei Co	52.88	4942	9 Nov	-0.52					10 May	1.40								181.41	1.93	I
31	Mapam Yumco	409.9	4585	13 Jan	0.00	22 Jan	0.04	20 Apr	0.13	29 Apr	-0.08	9.60	0.02	87.86	0.09	8.61	0.00	106.06	-0.08	II	
32	Margai Caka	145.17	4793	3 Nov	0.50**					26 May	-0.64								203.82	-1.15 [†]	I
33	Meiriqiecuomari	86	4947	31 Oct	-0.01					18 May	-0.58								198.65	-0.57	I
34	Nam Co	2040.9	4724	12 Jan	0.51					9 May	-0.21								116.59	-0.72	I
35	Ngangla Ringco	542.89	4716	9 Dec	0.75 [†]	27 Dec	0.51 [†]	14 Apr	0.30	1 May	0.10	18.76	-0.24	107.76	-0.21 [†]	16.65	-0.20	143.18	-0.65	I	
36	Ngangze Co	445.48	4685	4 Dec	1.25**	11 Dec	1.04	18 Mar	1.42	2 Apr	0.42	7.43	-0.15	96.50	0.38	15.18	-0.80	119.12	-0.82	I	
37	Ngoring Lake	629.75	4267	1 Dec	0.25					8 May	-0.02								158.00	-0.27	IV
38	Palung Co	144.65	5101	30 Nov	0.18	8 Dec	0.31	20 Apr	-0.34	8 May	-0.20	7.94	0.12	132.47	-0.65	18.65	0.14	159.06	-0.38	I	
39	Puma Yumco	294.11	5013	1 Jan	0.41					1 May	-0.54								120.24	-0.95	I
40	Pung Co	172.11	4529	20 Dec	0.75**					12 Apr	-0.29								113.59	-1.05	I
41	Qinghai Lake	4254.9	3194	18 Dec	0.40	6 Jan	0.49	23 Mar	-0.50	4 Apr	-0.07	18.59	0.09	76.82	-0.99**	11.94	0.43	107.35	-0.47	IV	
42	Rola Co	82.52	4815	5 Nov	-0.36					25 May	1.24								200.59	1.60	I
43	Selin Co	2129.02	4539	19 Dec	0.71 [†]	5 Jan	0.55	4 Apr	0.15	18 Apr	-0.56	16.29	-0.17	89.71	-0.39	13.76	-0.71**	119.76	-1.27 [†]	I	
44	Sugan Lake	101.4	2793	18 Nov	0.10	29 Nov	0.51	28 Mar	0.33	10 Apr	0.13	10.59	0.41	119.12	-0.19 [†]	13.59	-0.20	143.29	0.02	III	
45	Taiyang Lake	101.82	4881	22 Nov	0.46 [†]					18 Jun	0.56								207.65	0.10	III
46	Taro Co	486.62	4567	19 Jan	0.16					15 Apr	-0.40								86.59	-0.56	I
47	Telashi Lake	63.15	4805	4 Nov	0.19					27 May	0.86								203.94	0.67	I
48	Tu Co	428	4929	23 Nov	-0.52	1 Dec	-0.93 [†]	13 May	2.11 [†]	26 May	1.70**	8.47	-0.41	163.24	3.04	12.65	-0.41	184.35	2.22**	I	
49	Tuosu Lake	137.76	2805	24 Dec	0.17					25 Mar	-0.06								90.24	-0.23	III
50	Urru Co	362.52	4554	3 Jan	0.01					22 Apr	0.48								109.00	0.47	I

51	Xuejing Lake	72.73	4807	22 Oct	0.64**				11 Jun	-0.26									232.47	-0.91	I
52	Xuemei Lake	41.33	4873	26 Oct	0.30				24 Jun	0.34									240.94	0.04	I
53	Yaggain Co	97.41	4534	7 Dec	1.48**				19 Apr	0.10									132.82	-1.38**	I
54	Youbucuo Lake	63.19	4640	20 Dec	0.56 [†]				15 Apr	-0.14									116.71	-0.70	I
55	Yuye Lake	126.36	4856	20 Oct	0.73**				14 Jun	-1.08									236.71	-1.81 [†]	I
56	Zhari Namco	990.26	4612	27 Dec	0.64 [†]	7 Jan	0.48	31 Mar	0.74	13 Apr	0.63	10.41	-0.17	83.29	0.26 [†]	12.41	-0.11		106.12	-0.01	I
57	Zhaxi Co	47.47	4416	24 Nov	0.70**				13 Apr	-0.89**									139.71	-1.59**	I
58	Zige Tangeo	225.55	4568	9 Dec	1.01**	15 Dec	0.94**	9 Apr	-0.17	24 Apr	-0.12	5.53	-0.07	115.47	-1.11 [†]	14.88	0.05		135.88	-1.13 [†]	I

856 *Note.* ^a Wan et al. (2014). ^b The altitudes of lakes are derived from Shuttle Radar Topography
857 (SRTM) digital elevation model (DEM) data
858 (<http://srtm.csi.cgiar.org/SELECTION/inputCoord.asp>). * Statistical significance at the 0.05
859 level (Mann-Kendall test). ** Statistical significance at the 0.01 level (Mann-Kendall test).

860

861

862

863

864

865

866

867 **Appendix B**

868 **Table B1.** *Lake Ice Phenology Statistics From 2001 to 2017 (FUS: Freeze-up Start, FUE:*
 869 *Freeze-up End, BUS: Break-up Start, BUE: Break-up End, FUD: Freeze-up Duration, BUD:*
 870 *Break-up Duration, CFD: Complete Freezing Duration, and ICD: Ice Cover Duration)*

	Mean ^a	Minimum	Maximum	Max-Min	Median	Standard deviation	
Mean date/days	FUS**	30 Nov	20 Oct (Yuye Lake)	19 Jan (Taro Co)	90.47	29 Nov	21.57
	FUE*	16 Dec	15 Nov (Hoh Xil Lake)	22 Jan (Mapam Yumco)	68.48	13 Dec	17.81
	BUS*	16 Apr	18 Mar (Ngangze Co)	12 Jun (Hoh Xil Lake)	86.60	10 Apr	22.78
	BUE**	6 May	25 Mar (Tuosu Lake)	7 Jul (Gozha Co)	104.00	1 May	26.62
	FUD*	9.81	3.94 (Lagkor Co)	18.76 (Ngangla Ringco)	14.82	8.76	4.56
	BUD*	13.01	7.29 (Dong Co)	18.65 (Palung Co)	11.35	13.00	2.92
	CFD*	121.12	76.82 (Qinghai Lake)	209.65 (Hoh Xil Lake)	132.82	117.06	35.53
	ICD**	157.78	86.59 (Taro Co)	240.94 (Xuemei Lake)	154.35	147.74	42.99
Change rate (d yr ⁻¹)	FUS	0.53	-1.22 (Lexiewudan Co)	1.48 (Yaggain Co)	2.70		0.52
	FUE	0.54	-0.93 (Tu Co)	1.04 (Ngangze Co)	1.97		0.43
	BUS	0.58	-0.50 (Qinghai Lake)	2.11 (Tu Co)	2.61		0.69
	BUE	0.54	-1.63 (Bangkog Co)	4.25 (Lexiewudan Co)	5.88		0.92
	FUD	0.18	-0.41 (Tu Co)	0.41 (Sugan Lake)	0.82		0.20
	BUD	0.30	-0.80 (Ngangze Co)	0.43 (Qinghai Lake)	1.24		0.35
	CFD	0.68	-1.13 (Lagkor Co)	3.04 (Tu Co)	4.17		0.97
	ICD	0.90	-2.73 (Bangkog Co)	5.46 (Lexiewudan Co)	8.20		1.32

871 *Note.* ^a The mean change rates of lake ice phenology are mean absolute values. * Calculated from
 872 18 lakes. ** Calculated from 58 lakes.

873